Electron Spin Resonance of Biomolecules

Betty J. Gaffney
Department of Biological Sciences, BIO Unit 1, Tallahassee, FL, USA

Keywords

cwESR
ESR signal detected with radiation turned on continually during recording.

EPR, PMR, EMR
Synonyms, in practice, for ESR: electron paramagnetic resonance, paramagnetic resonance, and electron magnetic resonance.

EPRI
In vivo imaging based on the ESR signal of a paramagnetic molecule.

ESR
Electron Spin Resonance. Spectroscopy involving unpaired electrons in a magnetic field.

ENDOR
Electron-Nuclear Double Resonance spectroscopy. Spectroscopy in which NMR signals are observed as changes in intensity of ESR signals.

ESEEM
Electron Spin Echo Envelope Modulation spectroscopy. A pulsed ESR technique in which nuclear moments modulate time-dependent electron relaxation.

g-factor
Proportionality constant between ESR frequency applied and the magnetic field where ESR absorption occurs.

Hyperfine Splitting
An ESR signal of an unpaired electron is split into multiple signals, one for each dipolar interaction with a unique nuclear spin.

Isotropic or Anisotropic
Uniform or asymmetric, respectively, with regard to coordinates in space.

Pulsed ESR
ESR signal detected as a function of time after a pulse of energy.

Spin Label
Paramagnetic molecule used to provide information about a nonparamagnetic biomolecule with which it interacts; the same term is used in nuclear magnetic resonance imaging for manipulations of nuclei in a portion of the sample to amplify the NMR signal from localized regions.

Spin Trap
A means of capturing information from a radical that has a short lifetime or other properties rendering it unsuitable for ESR so that, when trapped, useful ESR signals result.

200300104

Electron spin resonance (ESR) refers to spectroscopy of unpaired electrons, and is sometimes called electron paramagnetic resonance (EPR) or electron magnetic resonance (EMR). The theoretical bases of ESR spectroscopy are similar to those of nuclear magnetic resonance (NMR), except that an electron spin, rather than a nuclear spin, is the focus. Unpaired electrons in biological systems are in much lower abundance than nuclei, so ESR is a technique that focuses on local sites while NMR is more global.

Two electrons are paired, with antiparallel spins, in a single chemical bond. The ESR requirement of an unpaired electron spin is met in biology when (1) a chemical bond is broken homolytically, as in formation of a free-radical enzyme intermediate; (2) there are unfilled valence orbitals, as there are in oxygen, nitric oxide, or many metal ions; and (3) one-electron oxidation or reduction of a nonparamagnetic biomolecule has occurred. Biological subjects for ESR include free-radical enzyme intermediates, metal ions, nitric oxide and some of its complexes, and redox-active cofactors such as quinones and flavins. The range of applications of ESR spectroscopy is not limited to natural sources of unpaired electrons. An ESR probe technique, site-directed spin labeling (SDSL), is widely applied to examine dynamics and folding of biomolecules. Other paramagnetic probes can be used to image oxygen or nitric oxide in biological tissues *in vitro* and *in vivo*.

1 Basic ESR Concepts and Spectra

The term "spin" in the designations of various forms of magnetic resonance spectroscopy refers to a property of electrons (or nuclei). It is the interaction of the spin with magnetic field that leads to separation of energy levels between which spectroscopic transitions occur. Usually, a magnetic field is required for ESR, as well as a source of energy to effect transitions, although a few spin transitions can be detected in the absence of an applied magnetic field.

ESR signals can be detected during continuous application of microwave energy of narrow bandwidth (continuous wave ESR, cwESR) or after a short, broader-band microwave pulse (pulsed ESR). In the former case, the signal is detected by scanning the external magnetic field through the resonance condition; in the latter, the field is fixed for each pulse, but, because of the breadth of many ESR signals, data may be collected at multiple steps in magnetic field. To filter noise, a cwESR signal is recorded with an additional magnetic field modulation and phase-sensitive detection, resulting in an output that is the derivative of the absorption. Absorption and derivative ESR signals are illustrated in Figs. 1(a, b).

Equation (1) gives the resonance condition for a free electron, where ν is the microwave frequency; g_e is Zeeman splitting constant for a free electron; β_e, the Bohr magneton, is proportional to the charge to mass ratio of the electron; and B_0 is the external magnetic field in which the sample resides.

$$\text{Energy} = h\nu = g_e \beta_e B_0 \qquad (1)$$

Internal magnetic fields in molecules alter the simple spectrum shown in Fig. 1(b)

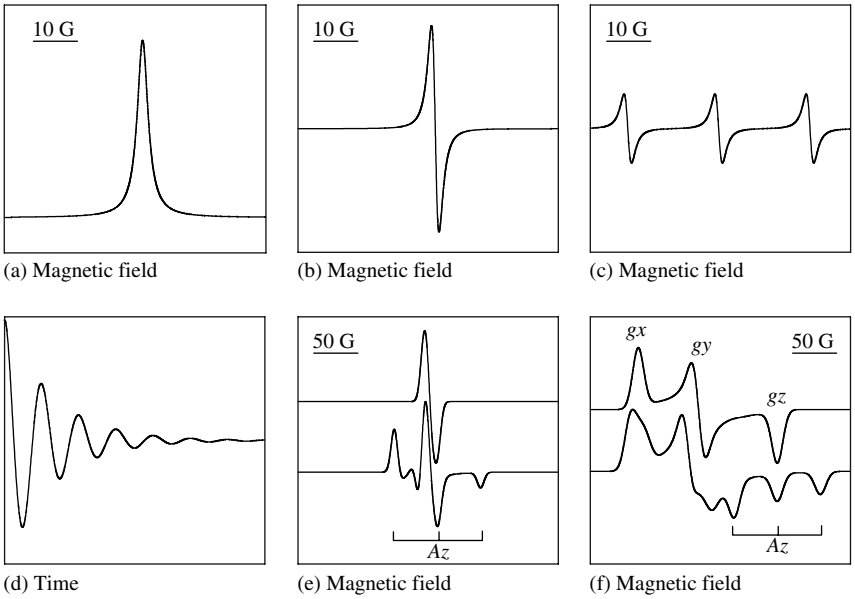

Fig. 1 Basic ESR spectra concepts are illustrated. (a) An isolated, unpaired electron has an absorption ESR signal of Lorentzian shape; (b) in cwESR, the signal shown in (a) is recorded as the derivative of the absorption; (c) when a nuclear spin interacts with the unpaired electron, the signal is split into multiple lines, one for each nuclear spin state (^{14}N spin states are −1, 0, and +1); (d) the time-dependent response of an unpaired electron to a pulse is an oscillating decay; (e) and (f) are spectra with parameters typical of spin labels recorded at 9.4 GHz (e) and 94 GHz (f). In (e) and (f), the upper spectra are calculated with only *g*-factor anisotropy, while the calculations of the lower spectra include anisotropic terms for both *g*-factor and hyperfine splitting. The largest hyperfine splitting, *Az*, is shown.

and thus provide the features that allow information about structure and dynamics to be deduced. The local magnetic fields add terms to Eq. (1), and it is convenient to refer to the proportionality between the frequency applied and the magnetic field at which a characteristic feature is seen in the ESR spectrum in terms of an ''effective *g*-factor,'' g', as given in Eq. (2).

$$h\nu = (g_e \beta_e B_0 + \text{other terms}) = g' \beta_e B_0 \quad (2)$$

The ''other terms'' include, but are not limited to, those of electron spin dipolar interactions with spins of nuclei or other unpaired electrons, spin exchange due to overlap of the orbitals of two electron spins, and terms arising from strong interactions of multiple electrons residing on the same atom. Different terms dominate the ESR spectrum in varied applications. Some terms are described by expressions including magnetic field and other terms are independent of magnetic field. ESR spectra obtained at several different frequencies, ν, help resolve contributions of the different terms.

Dipolar interactions of magnetic nuclei (for instance, hydrogen or nitrogen) with an unpaired electron render ESR spectra sensitive to molecular structure. An unpaired electron residing in a p- or π-orbital on ^{14}N, such as occurs in a spin label or in nitric oxide (NO), has dipolar interactions

of slightly different energies with each of the nitrogen nuclear spin states (^{14}N nuclear spins −1, 0, and +1). As a result, the simple unpaired electron ESR signal becomes a spectrum with three lines, each of one-third the intensity (Fig. 1(c)) of the single line (Fig. 1(b)). The separation of the lines is termed the *hyperfine splitting* of the electron spin by the nuclear spins. Hyperfine splitting by ^{1}H or ^{15}N yields ESR spectra divided into two lines.

The response of spins to a short pulse of energy is recorded over time in pulsed ESR. The time-dependent response may be converted to the cwESR spectrum by Fourier transformation. A Fourier transform of the absorption signal (Fig. 1(a)), which would be detected in the pulsed experiment, is shown in Fig. 1(d). The exponential decay is related to the line width and the oscillations to the offset of the absorption peak from zero magnetic field. ESR and NMR are connected in the variations of pulsed ESR that are termed electron spin echo envelope modulation (ESEEM) and electron-nuclear double resonance (ENDOR), in which electron transitions are modulated by nearby nuclei. After Fourier transformation of the time response, the characteristic frequencies of nuclear spins near the electron spin are displayed in these experiments. Determining the nature, geometric arrangement, and distance of nuclei from the unpaired electron are applications of these pulsed ESR techniques.

Figures 1(a, b) are based on a fictitious "free electron." In a molecule, an unpaired electron responds to an anisotropic (asymmetric) environment, resulting in energies for the magnetic interactions that depend on the orientation of each molecule in the magnetic field. The *g*-factor becomes a matrix (**g**) relating the vectors of magnetic field, B_0, and electron spin, *S*. The expression of the energy for the hyperfine interaction is $S\,\mathbf{A}\,I$, where electron and nuclear spin vectors are *S* and *I*, respectively, and **A** is the interaction matrix. The diagonal elements of the **g**- and **A**-matrices are *gx*, *gy*, and *gz* and *Ax*, *Ay*, and *Az*, respectively. As a result of these interactions, if a frozen solution is studied, the spectrum will be the sum of spectra from molecules at all orientations, and will be broader than the free electron signal. Figures 1(e, f) illustrate the type of spectra that result from a frozen solution of nitroxide molecules. Figure 1(e) is calculated for a frequency of applied radiation (9.41 GHz) 10 times lower than that of Fig. 1(f) (94.1 GHz). The upper spectra show only the contribution from the anisotropic *g*-factor. The features corresponding to *gx*, *gy*, and *gz* can hardly be seen in Fig. 1(e) (upper curve), but they are separated as indicated in Fig. 1(f) (upper curve). This is because the *g*-factor energy term depends on magnetic field. In contrast, the hyperfine term is constant. The lower curves indicate the *Az* component of the hyperfine splitting; it is centered on *gz*. *Ax* and *Ay* are smaller and are not indicated on the figures. However, it can be seen in Fig. 1(f) (lower curve) that the *gx* and *gy* regions are broadened by the smaller *Ax* and *Ay* hyperfine splittings.

2 ESR and the Roles of Naturally Occurring Paramagnetic Biomolecules

2.1 Free-radical Enzyme Intermediates

Cofactors and amino acid side chains are known to form radical, or paramagnetic intermediates in enzymes. Ribonucleotide reductases use a pathway of electron transfers to carry out reduction of

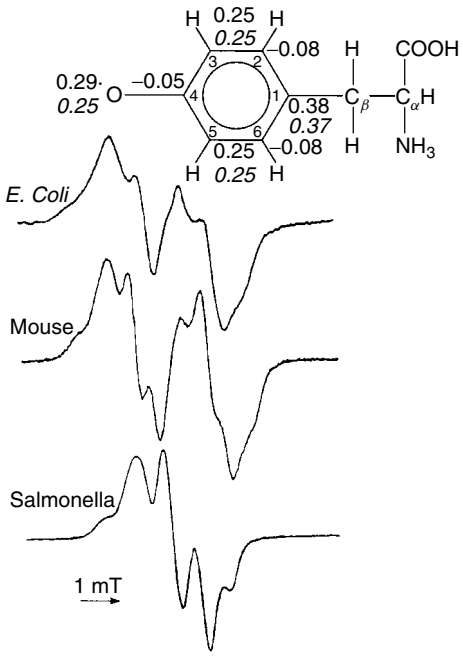

Fig. 2 ESR spectra of tyrosine free radicals of ribonucleotide reductase R2 subunits from different organisms. The ESR spectra at ~9 GHz were recorded at temperatures from 20 to 30 K. The numbers given on the structure are the spin density distributions for the *Escherichia coli* (Roman letters) and *Salmonella typhimurium* (italics) enzymes. (Reprinted with permission from Gräslund, A. and Sahlin, M. (1996) *Ann. Rev. Biophys. Biomol. Struct.* **27**, 259–286.)

ribonucleotides to deoxyribonucleotides. In the enzymes from different sources, the presence of free-radical intermediates on side chains of the amino acids tyrosine, tryptophan, cysteine, and even glycine has been demonstrated by ESR. ESR studies of tyrosine radicals, in this system and also in electron-transfer membranes, show that the unpaired electron density at the various carbon atoms of the tyrosine aromatic ring is fine-tuned by hydrogen bonds to the phenolic oxygen and by the protein environment. ESR spectra also provide information about side-chain torsion angles of the tyrosines giving rise to radicals. Figure 2 gives examples of EMR spectra of tyrosine radicals of ribonucleotide reductases from several sources.

In other proteins, tyrosine radicals participate in the mechanisms of cytochrome oxidase (mitochondrial respiratory complex IV), cyclooxygenase and other heme enzymes. In other proteins, glycine radicals have functional roles in lysine 2,3-aminomutase, pyruvate formate-lyase, and benzylsuccinate synthase. Enzyme-bound substrate and cofactor radical intermediates have also been characterized in enzymes dependent on S-adenosyl methionine, adenosylcobalamin, and arachidonic acid. It is often useful to use isotopic labeling with nuclei having magnetic moments (^{2}H, ^{13}C, ^{15}N, ^{17}O) in the effort to identify the radical site in an enzyme intermediate.

2.2 Paramagnetic Metal Ions in Biology

All metal ions containing unpaired electrons (paramagnetic ions) are, in principle, subjects for study by ESR, but the experimental conditions are quite varied. The paramagnetic ions in proteins, commonly studied by ESR, include manganese^{2+}, copper^{2+}, iron^{3+}, occasionally iron^{2+},

nickel^{3+}, vanadyl ($V = O^{2+}$), and cobalt^{2+}. The conditions for the spectroscopy differ drastically depending on which metal is the subject of study. Manganese ions are sometimes detected with high sensitivity in solutions at room temperature. However, detection of ^{17}O-threonine sidechain ligands to manganese in p21 *ras* required both low temperature and high-frequency ESR to give optimum results. Copper sites also can be detected at room temperature, but sensitivity is improved by conducting the ESR experiments at liquid nitrogen temperature or lower. Studies of iron are almost always done at temperatures near that of liquid helium. The two primary reasons that low temperature is used in metal ion ESR are that relaxation times are too fast for room temperature studies and the signal intensity increases inversely with temperature. The pulsed ESR methods ENDOR and ESEEM are chosen to detect nuclei such as nitrogen or hydrogen bound to, or near, metal ion sites.

Quantitative evaluation of the number of unpaired spins in different sites within a complex biochemical electron-transfer system can be made by ESR and associated studies. For experiments of this type, both calculations of the theoretical spectra and a multifrequency approach in the experiments are needed for interpretation. Recent advances in high-frequency ESR provide improved resolution in samples with multiple ESR-detectable metal sites. For example, Fig. 3 shows a high-frequency ESR spectrum of a frozen solution of copper ion in the site normally occupied by iron in lactoferrin.

The copper spectrum, spread over the field region from ~2.9 to 3.3 T, is well separated from the six-line signal of a manganese impurity near 3.4 T. At lower ESR frequencies, the manganese signal is superimposed on the central portion of the copper signal. Also notable in the high-frequency ESR spectrum shown (Fig. 3) is that the portion (at 2.9–2.95 T) of the spectrum arising from molecules with a unique axis aligned close to the magnetic field direction is well separated from the portion (at 3.2–3.3 T) arising from molecules in which this axis is perpendicular to the field. Additionally, the

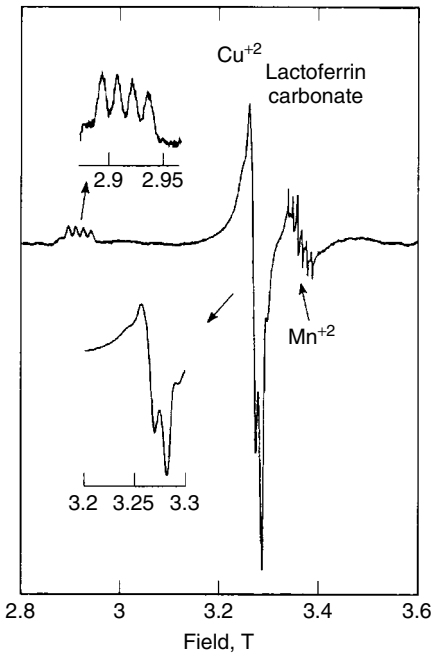

Fig. 3 High-frequency ESR spectrum of dicupric lactoferrin. The spectrum was recorded at 40 K and 94.1 GHz. The two regions from which significant information can be obtained are amplified in insets on the left. The feature on the right is the ESR signal from an impurity of manganese ion in the sample. (Reprinted with permission from Gaffney, B.J., Maguire, B.C., Weber, R.T., Maresch, G.G. (1999) Disorder at metal sites in proteins: a high frequency EMR study, *Appl. Magn. Res.* **16**, 207–222.)

splitting of these regions into four features arises from interaction of the unpaired electron with the four nuclear spin states of the copper nucleus. For copper proteins, very low-frequency EPR is also useful in revealing how many nitrogen ligands to the metal there are. This approach, as well as pulsed ESR, helped elucidate the nature of multiple copper binding sites in the prion protein (PrP), for example.

2.3 Protein Complexes with Nitric Oxide (NO)

Nitric oxide (NO) is a paramagnetic gas and molecular adducts of NO in solution give ESR signals that are employed to determine the pathway of nitric oxide transfers in proteins or the location of NO in tissues by *in vivo* ESR imaging. The characteristic ESR signal of some NO complexes is three lines, broader but otherwise similar to the spectrum shown in Fig. 1(c). When the ^{15}N isotope (nuclear spin states $\pm 1/2$) is incorporated in NO, the ESR spectrum simplifies to two lines. In an NO complex with iron, copper or other metals in proteins, broader signals with no resolved hyperfine splitting may or may not be observed. Three-line hyperfine splitting is seen in NO complexes with 5-coordinate ferrous heme iron, with the NO spin traps: ferrous ion chelated with dithiocarbamate derivatives, and with diverse iron-sulfur-dinitrosyl species *in vivo*.

NO is often used biochemically as an oxygen mimic, but it binds more tightly to metal centers than O_2 does and may alter other ligand geometries. When a single NO combines with ferrous iron, an ESR-detectable complex is formed. The spin 1/2 of NO combines with the even spin (spin = 0 or 2) of ferrous iron to give half-integer spin for the complex (spin = 1/2 or 3/2). Generally, half-integer spins yield well-resolved ESR spectra, whereas spin = 0 is not paramagnetic, and spin = 2 usually does not give resolved signals.

The strength of the Fe–NO interaction with iron in hemoglobin is demonstrated under conditions in which hemoglobin binds NO preferentially at the α-subunits; here, NO acts transaxially to cleave the proximal iron-His bond. ESR spectra of the resulting five-coordinate α-subunit heme have three resolved peaks from ^{14}N-hyperfine interactions. A similar spectrum of the five-coordinate NO complex with heme in myoglobin is shown in Fig. 4.

In contrast, when NO is in a six-coordinate complex with ferrous heme, a broad ESR signal, without hyperfine, is observed. NO activation at heme in guanyl cyclases also involves breaking an Fe-His bond, and the NO-Fe complex is ESR detectable. Interaction of NO or nitrite with oxyhemoglobin, or with methemoglobin, leads to a third species, S-nitrosyl hemoglobin. NO also reacts with

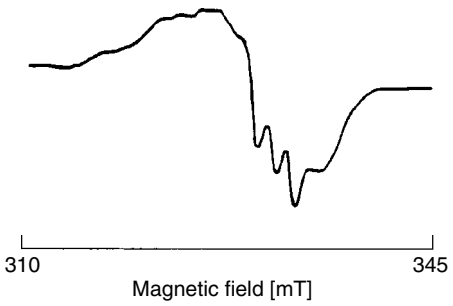

Fig. 4 The ESR spectrum of deoxymyoglobin to which nitric oxide (NO) gas was added. The spectrum was recorded at 77 K and a frequency of 9.1 GHz. (Reprinted with permission from Singel, D. J., Lancaster, J. R. Jr., (1996) *Methods in Nitric Oxide Research*, Feelisch, M., Stamler, J. S. (Eds.) John Wiley & Sons Ltd Ch. 23, pp. 341–356.)

the iron in iron-sulfur proteins. In the case of aconitase, one iron of the 4Fe-4S is lost upon reaction with NO and ESR signals of a protein-bound iron-$(NO)_2$ complex can be seen. This complex is likely an intermediate in the conversion to 3Fe-4S apoaconitase.

2.4 Factors Directing Electron Flow in Energetic Membranes

Mitochondrial and photosynthetic membranes are rich in species giving ESR signals during electron transfer. The full range of recent chemical bonding theory and ESR instrumentation is brought to bear in determining the electron-transfer pathways through the multiple intermediates. ESR studies provide electronic structures of intermediates in electron-transfer pathways, including electron spin density around the ring of an aromatic radical and the overlap of electron orbitals between two paramagnetic intermediates. This information is essential for determining how the surrounding protein matrix influences the path that electrons follow from one paramagnetic intermediate to another. Key electron-transfer species that are observed by ESR methods are summarized in Table 1. The list is not comprehensive. ESR examines the species listed either individually, or in pairs.

2.4.1 ESR Studies of Photosynthesis

The components of photosynthetic electron-transfer pathways, chlorophylls, quinones, and metal ions, are selected for ESR studies by preparations that include optical excitation, selective depletion of some components, and molecular biology. Because electron transfer can be primed by optical excitation in the preparations, it is possible to trap very short-lived intermediates by optical excitation of low-temperature glasses. High-frequency ESR is applied in some cases to improve resolution of ESR spectral components, much as higher frequency NMR gives better resolution of different nuclei (see also Sect. 2.2). In bacterial reaction centers, electrons flow from an excited bacteriochlorophyll dimer to bacteriopheophytin, to quinone A (Q_A), and to quinone B (Q_B). The electronic interactions between these sites are influenced by a $^{2+}$Fe ion on the pathway.

Tab. 1 Some Components of Energetic Membranes Detected by ESR.

Component	*Abbreviation*	*Membrane*
Donor cation (a chlorophyll)	$BChl_2$, $P_{700}^{+\bullet}$ chlorophyll b, $P_{680}^{+\bullet}$	RC, PS I, PS II
Reduced quinones	$Q_A^{-\bullet}$, $Q_B^{-\bullet}$, $Q^{-\bullet}$	RC, PS I, PS II
Iron-sulfur clusters	$[2Fe2S]^{-1}$, $[4Fe4S]^{-1}$, or $[4Fe4S]^{+3}$	PS I, Fd, Cplx III
Manganese clusters	Mn(III) + 3 Mn(IV)	PS II-S_2
Tyr radical	$Tyr^{+\bullet}$	PS II
Ferric heme	heme-Fe^{3+}	Cplx IV
Copper	Cu^{2+}	Cplx IV

Notes: RC: reaction center of purple bacteria; PS I: photosystem I of plants, cyanobacteria, green sulfur bacteria, and algae; PS II: photosystem II of plants, cyanobacteria, and algae; Fd: ferrodoxin; Cplx: one of the electron-transfer complexes of mitochondria; PS II-S_2: the S_2 intermediate of PS II photocycle.

Distances between electron sites on the intermediates, and the term describing electron exchange interactions between them, have now been tabulated for the bacterial system. Good agreement between these ESR measurements and electron-transfer theory is observed.

In plant photosynthetic membranes, ESR is used to examine the manner in which electrons flow ultimately into the photosynthetic oxygen-evolving complex that contains varied numbers of unpaired electrons associated with a cluster of four manganese atoms. A tyrosine radical abstracts an electron and a proton from the manganese cluster and water in steps, leading to oxygen evolution. Determining how the protein environment influences the electronic structure of the tyrosine radical and its coupling to the manganese cluster are subjects of study by the pulsed ESR techniques ESEEM and ENDOR.

2.4.2 ESR Studies of Respiratory Enzymes

In the synthesis of ATP, the mitochondrial respiratory chain employs many of the same cofactors as photosynthetic membranes, although the electron/proton transfers are not photochemically initiated. Instead, reductants or oxidants are used to isolate states with unpaired electrons. ESR contributes to understanding the electronic structure of the oxidized or reduced cofactors. In one example, ESR studies reveal an asymmetric hydrogen-bonding environment for a ubisemiquinone ($Q^{-\bullet}$) bound to bacterial quinol oxidase (QOX), bo_3. QOX is structurally and functionally related to mammalian cytochrome oxidases. In these experiments, quinones, ^{13}C-labeled individually at the carbonyl carbons, were substituted for the natural ubiquinone in QOX by detergent extraction and reconstitution. Control ESR experiments (^{14}N-ESEEM) demonstrated that the reconstituted, labeled quinones had the same hydrogen-bonding environment as native quinones. The line widths of the high-frequency ESR spectra from ^{13}C-labeled quinones differed, depending on whether the label was located on carbonyl-1 or -4. This shows that the unpaired electron spin distribution is asymmetric in the ubiquinone radical when the radical is bound to its cognate protein. The spin distribution is, in turn, related to an asymmetric hydrogen-bonding environment for the protein-bound $Q^{-\bullet}$.

3 ESR Probes of Biological Structure and Function

3.1 Spin Labeling

Nature does not always provide a free-radical ESR subject at a site of interest. Spin labels are stable, paramagnetic molecules that can be easily tailor-made by organic synthesis to provide selective structural and dynamical information via ESR spectroscopy. Most spin labels are nitroxide molecules. An advantage of spin label ESR studies is that they can be carried out at physiologically relevant temperatures and they are therefore sensitive to molecular motion. Nitroxide labeled nucleic acids, lipids, and enzyme cofactors are among the variations of spin label analogs that have been made. The largest area of applications to proteins is a molecular biology–based approach called site-directed spin labeling (SDSL) for studying the dynamics, folding, and structure of proteins.

3.1.1 Dynamics of Proteins, DNA, and Membranes

The effects of motion of a spin labeled macromolecule can be observed indirectly,

as averaging of features in the ESR spectrum or directly, by time domain ESR experiments. Effects of motion on a spin label ESR spectrum arise because the unpaired electron in the nitroxide molecule is in an asymmetric environment that renders the magnetic interactions sensitive to the orientation of the spin label in the field. When the spin label is rigidly attached to a larger molecule, ESR spectra reflect the motion of the macromolecule. The frequency of the particular ESR spectrometer used and the details of the detection scheme determine the timescale of motions that can be detected using spin label ESR. Motions occurring on timescales from milliseconds to fractions of a nanosecond have been measured. Applications in the area of dynamics include resolving spectra from distinct motional states of muscle, detecting time-dependent structural changes in bacteriorhodopsin, studies of the persistence length for DNA bending and measurements of anisotropic motion of lipids in membranes.

Figure 5 illustrates the sensitivity of ESR to spin label motion in an isotropic paraffin liquid and in a lipid membrane. The nitroxide molecules pictured have shapes that are roughly a sphere, a rectangular prism, and a long cylinder. The three peaks of equal intensity in ESR spectra of the spherical molecule, TEMPO (2,2,6,6-tetramethyl-4-ketopiperidine-1-oxygl), rotating in paraffin are characteristic of isotropic motion. The other spin labels move in paraffin with only slightly different rates about x, y, and z molecular axes (slight broadening of the third peak results). In contrast, motion of the larger spin labels is quite restricted in a lipid bilayer, as indicated by the broader ESR spectra. ESR of the fatty acid spin label reveals that the molecule rotates about the bilayer normal and has some internal flexibility. The lower spectrum from TEMPO in membranes was obtained from a more dilute lipid preparation than the upper one. The additional peak results from some TEMPO in water.

3.1.2 Site-directed Spin Labeling (SDSL)

In SDSL, a reactive nitroxide (e.g. a methanethiosulfonate) reacts with a cysteine side chain that has been placed at one or more selected sites in a protein by site-directed mutagenesis. Figure 6 shows the reaction scheme most often used in the SDSL approach. Secondary structure determination is one application of SDSL, and the approach involves stepwise substitution of nitroxides on a protein structural element. The surface exposure of the SDSL sites is determined through magnetic effects of oxygen or paramagnetic ions on ESR spectra. Interresidue distances between two spin label sites can also be determined as illustrated in Fig. 7 for phage T4 lysozyme. The overall structure of the protein shown in (a) indicates the close proximity of the two spin label side chains at residues 3 and 71. The inset (b) shows ESR spectra of folded, di-spin labeled phage lysozyme (bottom) and the same protein unfolded in urea (top). Spin labels separated by 10 to 25 Å give broadened spectra from which the interresidue distance can be determined. Once a protein derivative has been prepared with two interacting spin labels, spectral changes may be employed to determine refolding kinetics as illustrated in Fig. 7(c). Interresidue distances in membrane proteins, such as rhodopsin, are estimated by the complementary techniques of cysteine-scanning mutagenesis and paired site-directed spin labeling.

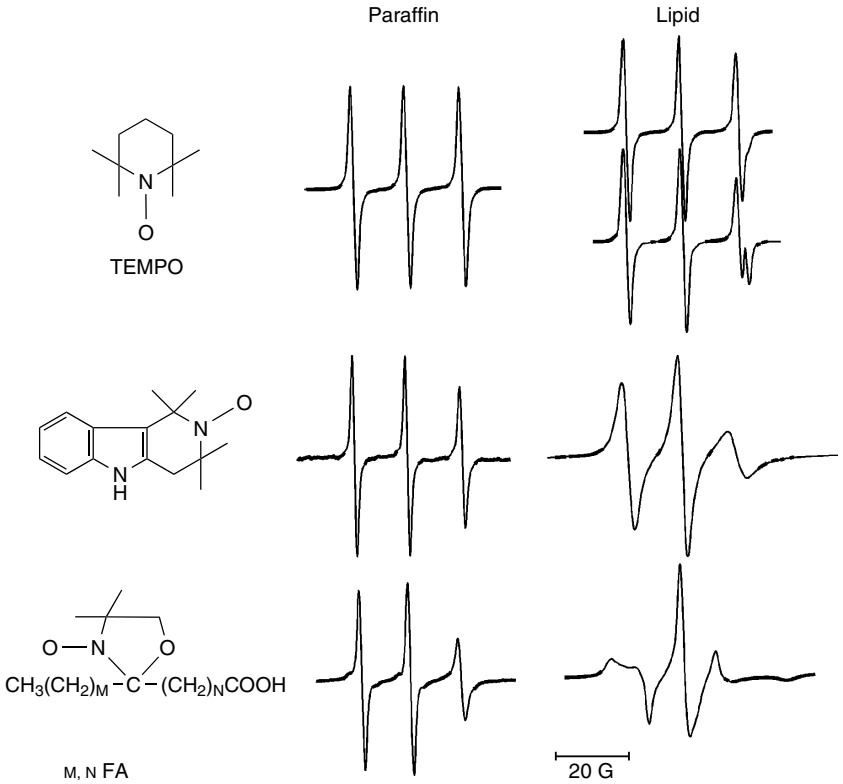

Fig. 5 The effects of restricted motion on the ESR spectra of molecules of different shapes and sizes. The spectra in the left column were obtained using a liquid paraffin solvent (isotropic) and those in the right column were with lipid bilayers (anisotropic fluid), both at 37 °C. Two concentrations of lipid were used for the upper right pair of spectra, a higher concentration in the top and a lower on below. (Redrawn with permission from Gaffney, B.J., Chen, S.C. (1977) *Methods in Membrane Biology*, Korn, E.D. (Ed.) Plenum Press, New York, Vol. 7, pp. 291–353.)

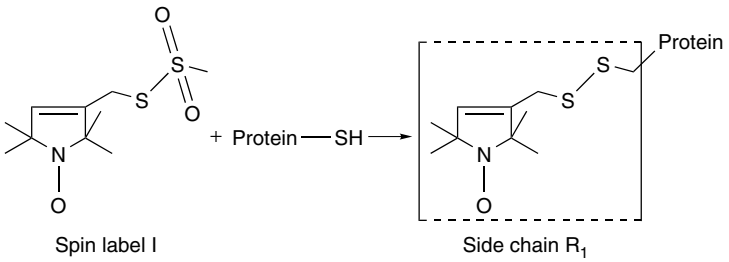

Fig. 6 Introduction of a site-directed spin label. A methanethiosulfonate spin label reacts with the natural, or genetically engineered thiol side chain of a protein to give a site-directed, spin-labeled protein. (Redrawn with permission from Hubbell, W.L., Mchaourab, H.S., Altenbach, C., Lietzow, M.A. (1996) Watching proteins move using site-directed spin labeling, *Structure* **4**, 779–783, Fig. 1.)

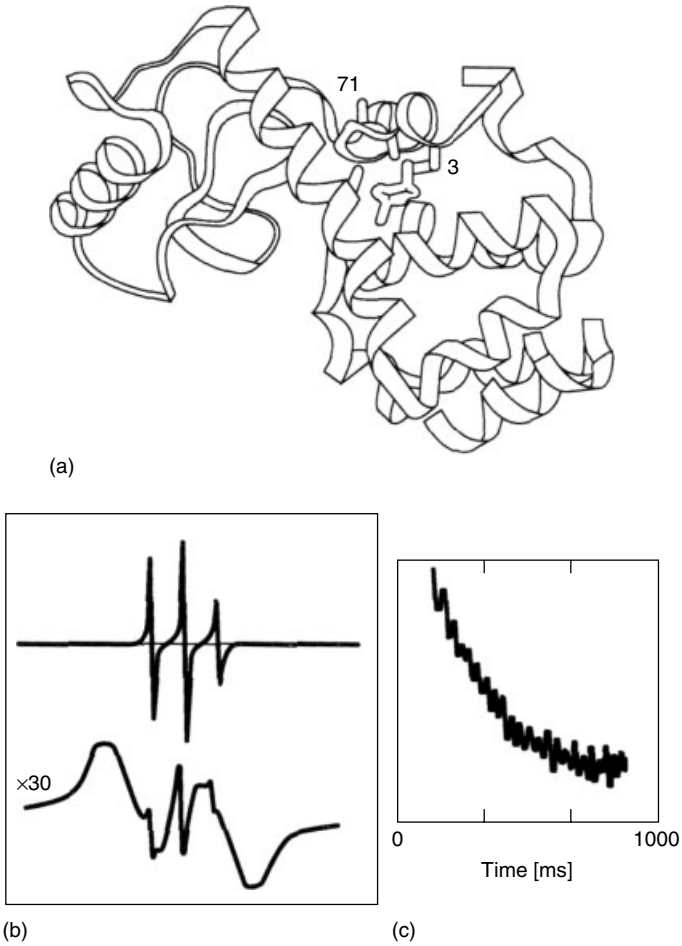

Fig. 7 Spin labeling of phage T4 lysozyme. The structure of a mutant T4 lysozyme in which two free cysteine residues were introduced (I3C and V71C) after reaction with spin labels is shown after reaction with spin labels, as in the scheme of Fig. 6. The proximity of the spin labels leads to the broad ESR spectrum shown in red in the inset (b, lower). The ESR spectrum of the same sample unfolded in urea is sharp and shows little interaction between spin labels (b, upper). The time-resolved rate of refolding can be followed by ESR (c). (Reproduced with permission from Hubbell, W.L., Mchaourab, H.S., Altenbach, C., Lietzow, M.A. (1996) Watching proteins move using site-directed spin labeling, *Structure* **4**, 779–783, Fig. 5.)

3.2 Spin Trapping

Detection of free radicals that occur transiently in cells places perhaps the most challenging demand on ESR, because the radicals have short lifetimes and are of low abundance. Free radicals can be detected indirectly by trapping them to give a longer-lived, secondary radical

in the technique called spin trapping. This technique usually employs nitroxide synthetic precursors to trap unstable free radicals such as xenobiotic radicals, superoxide, and hydroxyl radical. When there is one hydrogen on the carbon next to the nitrogen of a spin trap, the hyperfine splittings in ESR signals of the trapped radical are sensitive to whether an oxygen- or carbon-centered radical was trapped. The scheme below gives the chemistry of a spin trap nitrone reacting with trichloromethyl radical, derived from carbon tetrachloride. This approach has been used to trap similar radicals from halothane *in vivo*.

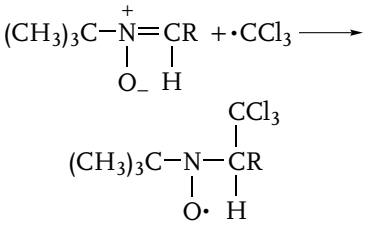

Spin traps can exhibit therapeutic effects *in vivo*, for instance, by inhibition of lipoprotein oxidation. Immunological methods are also used to detect spin-trapped sites on biomolecules.

3.3 ESR Imaging

Relaxation of spins is a dominant theme in ESR because the lifetimes of spins excited to upper energy levels are typically of the order of microseconds. A window on biological rates from 10^9 to about 100 s^{-1} results from the effects of magnetic relaxation on ESR spectra. Collision frequencies of molecules in solution, at biological concentrations, are in the range suitable for ESR relaxation responses. Relaxation of a spin probe depends on the frequency of collisions with paramagnetic oxygen. The simplest manifestation of relaxation is a change in line width of the ESR signal. This interaction is exploited to create images of oxygen levels in tissues. Spin traps selective for NO provide another basis for ESR imaging.

3.3.1 ESR Imaging of Oxygen in Tissues

The ESR spectrum of dissolved oxygen is not suitable for sensitive detection, but the ESR line width of a spin probe does respond to physiological concentrations of oxygen. EPR imaging, a technique under development, relies on spin probe relaxation to provide information about spatial distribution of oxygen in tissues, for instance, in tumors. In a sense, ESR imaging of oxygen concentration in tissues is a spin trap experiment in which the magnetism of oxygen is "trapped" through its magnetic, but not chemical, interactions with a stable spin probe. The degree of broadening of the ESR signal is transformed into an image.

A direct comparison of images of the same mouse tumor obtained by ESR imaging (EPRI) and by MRI has been made. In the experimental design, the leg bearing the tumor is centered in an ESR resonator or an MRI coil for the two imaging modalities. Paramagnetic reagents are applied intravenously in the ESR experiment, at a level similar to that used for MRI contrast agents. Both stable trityl (triphenylmethyl) radicals and nitroxides are used in EPRI, but the extremely narrow signal from trityl probes provides spatial resolution of about 1 mm in a tumor of $7 \times 7 \times 10$ mm. An ESR spectrum of the reagent in each pixel is obtained (spectral-spatial imaging). Separate calibration experiments demonstrate linear response of the ESR line width to oxygen concentration in the range 0 to 75 torr $\pm \sim 3$ torr. ESR and MRI obtain

comparable images of regions of the spatial distribution of oxygen, but the ESR experiment has the advantage that the oxygen concentrations are measured quantitatively. ESR imaging is performed at low frequency because the higher frequencies used in most ESR spectroscopy cannot penetrate far into wet tissues.

3.3.2 ESR Imaging of NO

A focus of ESR imaging has been to examine formation of NO from nitrite in ischemic rat hearts. With increasing durations of ischemia, the myocardial pH drops and this facilitates reduction of nitrite to NO. For example, both *ex vivo* and *in vivo* experiments are conducted in hearts loaded with ~1 mM nitrite and the NO spin trap, ferrous (N-methyl-D-glucamine dithiocarbamate)$_2$. By comparing pH measurements from ^{13}P-NMR with the quantity of trapped NO in the heart, significant NO formation from nitrite is demonstrated. Control experiments with inhibitors of nitric oxide synthase (NOS) and cytochrome oxidase augment these experiments.

3.4 Long-range Distance (6–60 Å) Measurements by ESR

The influence by one spin on the relaxation of another can also extend over a distance. In practice, this makes it possible to measure, by ESR, the distance between two paramagnetic centers, separated by up to 60 Å, in a biomolecule.

The advantages of using ESR methods to measure selected nonbonding distances in biomolecules are that the measurements are usually free of paramagnetic sites other than those involved in the measurement, and the sample can be opaque or semisolid. Recently, methods for ESR distance measurement have been tested and refined. The choice of a method depends on the relative relaxation rates of the two paramagnets between which a distance is sought. Generally, organic radicals such as spin labels and tyrosine radicals have spins with slow relaxation rates, whereas metal ion spins relax faster. Thus, specific methods are chosen for cases in which a slow relaxer is paired with either a second slow, or second fast relaxing paramagnetic species. The range 6 to 60 Å is a conservative estimate of distances that can be determined by ESR studies of two interacting paramagnets.

Bibliography

Books and Reviews

Berliner, L.J., Eaton, G.R., Eaton, S.S. (Eds.) (2001) Distance measurements in biological systems by EPR, *Biological Magnetic Resonance*, Vol. 19, Plenum Press, New York, and earlier volumes in this series.

Cammack, R. (Ed.) (1985) The applications of electron spin/paramagnetic resonance in biochemistry; a colloquium in honor of Dr. Helmut Beinert, *Biochem. Soc. Trans.* **13**, 541–634.

Eaton, G., Eaton, S., Salikhov, K. (1997) *Foundations of Modern EPR*, World Scientific, Singapore.

Ehrenberg, A., Malmström, B.G., Vänngård, T. (1967) *Magnetic Resonance in Biological Systems*, Werner-Gren Center International Symposium Series, Vol. 9, Pergamon Press, Oxford.

Feher, G. (2002) My road to biophysics: picking flowers on the way to photosynthesis, *Annu. Rev. Biophys. Biomol. Struct.* **31**, 1–44.

Frey, P.A. (2001) Radical mechanisms of enzymatic catalysis, *Annu. Rev. Biochem.* **70**, 121–148.

Hubbell, W.L., Altenbach, C., Hubbell, C.M., Khorana, H.G. (2003) Rhodopsin structure, dynamics, and activation: a perspective from crystallography, site-directed spin labeling,

sulfhydryl reactivity, and disulfide cross-linking, *Adv. Prot. Chem.* **63**, 243–290.

McConnell, H.M., Gaffney-McFarland, B. (1970) Physics and chemistry and spin labels, *Q. Rev. Biophys.* **3**, 91–136.

Pilbrow, J.R. (1990) *Transition Ion Electron Paramagnetic Resonance*, Clarendon Press, Oxford.

Rosen, G.M., Britigan, B.E., Halpern, H.J., Pou, S. (1999) *Free Radicals: Biology and Detection by Spin Trapping*, Oxford University Press, Oxford.

Schultz, B.E., Chan, S.I. (2001) Structures and proton-pumping strategies of mitochondrial respiratory enzymes, *Annu. Rev. Biophys. Biomol. Struct.* **30**, 23–65.

Schweiger, A., Jeschke, G. (2001) *Principles of Pulse Electron Paramagnetic Resonance*, Oxford University Press, Oxford.

Weil, J.A., Bolton, J.R., Wertz, J.E. (1994) *Electron Paramagnetic Resonance, Elementary Theory and Practical Applications*, Wiley-Interscience, New York.

Primary Literature

Al'tshuler, S., Zavoisky, Y.K., Kozyrev, B.M. (1944) New method to study paramagnetic absorption, *Zhurn. Eksperiment. Teoret. Fiziki* **14**, 407–409.

Bar, G., Bennati, M., Nguyen, H.-H.T., Ge, J., Stubbe, J., Griffin, R.G. (2001) High-frequency (140-GHz) time domain EPR and ENDOR spectroscopy: the tyrosyl radical-diiron cofactor in ribonucleotide reductase from yeast, *J. Am. Chem. Soc.* **123**, 3569–3576.

Bellew, B.F., Halkides, C.J., Gerfen, G.G., Griffin, R.G., Singel, D.J. (1996) High frequency (139.5 GHz) electron paramagnetic resonance characterization of Mn(II)-H2^{17}O interactions in GDP and GTP forms of p21 *ras*, *Biochemistry* **35**, 12186–12193.

Burns, C.S., Aronoff-Spencer, E., Legname, G., Prusiner, S.B., Antholine, W.E., Gerfen, G.J., Peisach, J., Millhauser, G.L. (2003) Copper coordination in the full-length, recombinant prion protein, *Biochemistry* **42**, 6794–6803.

Calvo, R., Abresch, E.C., Bittl, R., Feher, G., Hofbauer, W., Isaacson, R.A., Lubitz, W., Okamura, M.Y., Paddock, M.L. (2000) EPR study of the molecular and electronic structure of the semiquinone biradical $Q_A^{-\bullet}$ $Q_B^{-\bullet}$ in photosynthetic reaction centers from *Rhodobacter sphaeroides*, *J. Am. Chem. Soc.* **122**, 7327–7341.

Calvo, R., Isaacson, R.A., Abresch, E.C., Okamura, M.Y., Feher, G. (2002) Spin-lattice relaxation of coupled metal-radical spin-dimers in proteins: application to Fe^{2+}-cofactor ($Q_A^{-\bullet}$, $Q_B^{-\bullet}$, $\phi^{-\bullet}$) dimers in reaction centers from photosynthetic bacteria, *Biophys. J.* **83**, 2440–2456.

Canaan, S., Nielsen, R., Ghomashchi, F., Robinson, B.H., Gelb, M.H. (2002) Unusual mode of binding of human Group IIA secreted phospholipase A2 to anionic interfaces as studied by continuous wave and time domain electron paramagnetic resonance spectroscopy, *J. Biol. Chem.* **277**, 30984–30990.

Carmieli, R., Manikandan, P., Kalb, A.J., Goldfarb, D. (2001) Proton positions in the Mn^{2+} binding site of concanavalin A as determined by single-crystal high-field ENDOR spectroscopy, *J. Am. Chem. Soc.* **123**, 8378–8386.

Cooper, C.E. (Ed.) (1999) Collected papers on biochemistry of nitric oxide, *Biochim. Biophys. Acta Bioenergetics* **1411**, 215–488.

Davydov, R., Makris, T.M., Kofman, V., Werst, D.E., Sligar, S.G., Hoffman, B.M. (2001) Hydroxylation of camphor by reduced oxycytochrome P450cam: mechanistic implications of EPR and ENDOR studies of catalytic intermediates in native and mutant enzymes, *J. Am. Chem. Soc* **123**, 1403–1415.

Debus, R.J., Campbell, K.A., Gregor, W., Li, Z.-L., Burnap, R.L., Britt, R.D. (2001) Does histidine 332 of the D1 polypeptide ligate the manganese cluster in photosystem II? An electron spin echo envelope modulation study, *Biochemistry* **40**, 3690–3699.

Devaux, P., McConnell, H.M. (1972) Lateral diffusion in spin-labeled phosphatidylcholine multilayers, *J. Am. Chem. Soc.* **94**, 4475–4481.

Eaton, S.S., Eaton, G.R. (2002) *Electron Paramagnetic Resonance Techniques for Measuring Distances in Proteins in Structures and Mechanisms: from Ashes to Enzymes*, ACS Symposium Series 827, American Chemical Society, Washington, DC, pp. 321–339.

Edwards, T.E., Okonogi, T.M., Robinson, B.H., Sigurdsson, S.T. (2001) Site-specific incorporation of nitroxide spin-labels into internal sites of the TAR RNA; structure-dependent dynamics of RNA by EPR spectroscopy, *J. Am. Chem. Soc.* **123**, 1527–1528.

Elas, M., Williams, B.B., Parasca, A., Mailer, C., Pelizzari, C.A., Lewis, M.A., River, J.N., Karczmar, G.S., Barth, E.D., Halpern, H.J. (2003) Quantitative tumor oxymetric images from 4D electron paramagnetic resonance imaging (EPRI): methodology and comparison with blood oxygen level-dependent (BOLD) MRI, *Magn. Reson. Med.* **49**, 682–691.

Fu, Z., Aronoff-Spencer, E., Backer, J.M., Gerfen, G.J. (2003) The structure of the inter-SH2 domain of class IA phosphoinositide 3-kinase determined by site-directed spin labeling EPR and homology modeling, *Proc. Natl. Acad. Sci. U. S. A.* **100**, 3275–3280.

Gaffney, B.J., Maguire, B.C., Weber, R.T., Maresch, G.G. (1999) Disorder at metal sites in proteins: a high frequency EMR study, *Appl. Magn. Res.* **16**, 207–222.

Gaffney, B.J., Marsh, D. (1998) High-frequency, spin label EPR of non-axial ordering and motion in cholesterol-containing membranes, *Proc. Natl. Acad. Sci. U. S. A.* **95**, 12940–12943.

Ge, M., Cohen, J.S., Brown, H.A., Freed, J.H. (2001) ARF6 binding to PIP2-containing vesicles creates defects in the bilayer structure: ESR studies on model membranes (2001), *Biophys. J.* **81**, 994–1105.

Gow, A.J., Benjamin, P., Luchsinger, B.P., John, R., Pawloski, J.R., David, J., Singel, D.J., Jonathan, S., Stamler, J.S. (1999) The oxyhemoglobin reaction of nitric oxide, *Proc. Natl. Acad. Sci. U. S. A.* **96**, 9027–9032.

Griffin, M., Muys, A., Noble, C., Wang, D., Eldershaw, C., Gates, K.E., Burrage, K., Hanson, G.R. (1999) XSophe, a computer simulation software suite for the analysis of electron paramagnetic resonance spectra, *Mol. Phys. Rep.* **26**, 60–84.

Griffith, O.H., McConnell, H.M. (1966) A nitroxide-maleimide spin label, *Proc. Natl. Acad. Sci. U. S. A.* **55**, 8–11.

Grimaldi, S., Ostermann, T., Weiden, N., Mogi, T., Miyoshi, H., Ludwig, B., Michel, H., Prisner, T.F., MacMillan, F. (2003) Asymmetric binding of the high-affinity QH-ubisemiquinone in quinol oxidase (bo_3) from *Escherichia coli* studied by multifrequency electron paramagnetic resonance spectroscopy, *Biochemistry* **42**, 5632–5639.

Halpern, H.J., Yu, C., Barth, E., Peric, M., Rosen, G.M. (1995) In situ detection, by spin trapping, of hydroxyl radical markers produced from ionizing radiation in the tumor of a living mouse, *Proc. Natl. Acad. Sci. U. S. A.* **92**, 796–800.

Hille, R., Olson, J.S., Palmer, G. (1979) Spectral transitions of nitrosyl hemes during ligand binding to hemoglobin, *J. Biol. Chem.* **254**, 12110–12120.

Hoffman, B.M. (2003) Electron-nuclear double resonance spectroscopy (And Electron Spin-Echo Envelope Modulation Spectroscopy) in bioinorganic chemistry, *Proc. Natl. Acad. Sci. U. S. A.* **100**, 3575–3578.

Högbom, M., Galander, M., Andersson, M., Kolberg, M., Hofbauer, W., Günter Lassmann, G., Nordlund, P., Lendzian, F. (2003) Displacement of the tyrosyl radical cofactor in ribonucleotide reductase obtained by single-crystal high-field EPR and 1.4-Å X-ray data, *Proc. Natl. Acad. Sci. U. S. A.* **100**, 3209–3214.

Hoogstraten, C.G., Grant, C.V., Horton, T.E., DeRose, V.J., Britt, R.D. (2002) Structural analysis of metal ion ligation to nucleotides and nucleic acids using pulsed EPR spectroscopy, *J. Am. Chem. Soc.* **124**, 834–842.

Hubbell, W.L., McConnell, H.M. (1968) Spin-label studies of the membranes of nerve and muscle, *Proc. Natl. Acad. Sci. U. S. A.* **61**, 12–16.

Hubbell, W.L., Mchaourab, H.S., Altenbach, C., Lietzow, M.A. (1996) Watching proteins move using site-directed spin labeling, *Structure* **4**, 779–783.

Hustedt, E.J., Beth, A.H. (2001) The sensitivity of saturation transfer electron paramagnetic resonance spectra to restricted amplitude uniaxial rotational diffusion, *Biophys. J.* **81**, 3156–3165.

Kennedy, M.C., Antholine, W.E., Beinert, H. (1997) An EPR investigation of the products of the reaction of cytosolic and mitochondrial aconitases with nitric oxide, *J. Biol. Chem.* **272**, 20340–20347.

Klett, R., Töring, J.T., Plato, M., Möbius, K., Bönigk, B., Lubits, W. (1993) Determination of the g-tensor of the primary donor cation radical in single crystals of *Rhodobacter sphaeroides* R-26 reaction centers by 3-mm high field EPR, *J. Phys. Chem.* **97**, 2015–2020.

Knecht, K.T., DeGray, J.A., Mason, R.P. (1992) Free radical metabolism of halothane *in vivo*: radical adducts detected in bile, *Mol. Pharmacol.* **21**, 943–949.

Kornberg, R.D., McConnell, H.M. (1971) Inside-outside transitions of phospholipids in vesicle membranes, *Biochemistry* **10**, 1111–1120.

LaConte, L.E.W., Voelz, V., Nelson, W., Enz, M., Thomas, D.D. (2002) Molecular dynamics simulation of site-directed spin labeling: experimental validation in muscle fibers, *Biophys. J.* **83**, 1854–1866.

Lendzian, F., Huber, M., Isaacson, R.A., Endeward, B., Plato, M. (1993) The electronic structure of the primary electron donor cation radical in *Rhodobacter sphaeroides* R-26: ENDOR and TRIPLE resonance studies on single crystals of reaction centers, *Biochim. Biophys. Acta* **1183**, 139–160.

McConnell, H.M. (1956) Effect of anisotropic hyperfine interactions on paramagnetic relaxation in liquids, *J. Chem. Phys.* **25**, 709–711.

McConnell, H.M., Chestnut, D.B. (1958) Theory of isotropic hyperfine interactions in π-electron radicals, *J. Chem. Phys.* **28**, 107–117.

Mustafi, D., Makinen, M.W. (1995) Structure, conformation, and probable mechanism of hydrolysis of a spin-labeled penicillin revealed by electron nuclear double resonance spectroscopy, *J. Am. Chem. Soc.* **117**, 6739–6746.

Norris, J.R., Uphaus, R.A., Crespi, H.L., Katz, J.J. (1971) Electron spin resonance of chlorophyll and the origin of signal I in photosynthesis, *Proc. Natl. Acad. Sci. U. S. A.* **68**, 625–628.

Persson, M., Harbridge, J.R., Hammarström, P., Mitri, R., Mårtensson, L.-G., Carlsson, U., Eaton, G.R., Eaton, S.S. (2001) Comparison of EPR methods to determine distances between spin labels on human carbonic anhydrase II, *Biophys. J.* **80**, 2886–2897.

Qin, P.Z., Hideg, K., Feigon, J., Hubbell, J.L. (2003) Monitoring RNA base structure and dynamics using site-directed spin labeling, *Biochemistry* **42**, 6772–6783.

Ramirez, D.C., Chen, Y.-R., Mason, R.P. (2003) Immunochemical detection of hemoglobin-derived radicals formed by reaction with hydrogen peroxide: involvement of a protein-tyrosyl radical, *Free Radical Biol. Med.* **34**, 830–839.

Reddy, T.J., Iwama, T., Halpern, H.J., Rawal, V.H. (2002) General synthesis of persistent trityl radicals for EPR imaging of biological systems, *J. Org. Chem.* **67**, 4635–4639.

Sefton, B.M., Gaffney, B.J. (1974) Effect of the viral proteins on fluidity of the membrane lipids in sindbis virus, *J. Mol. Biol.* **90**, 343–358.

Steinhoff, H.J., Mollaaghababa, R., Altenbach, C., Hideg, K., Krebs, M., Khorana, H.G., Hubbell, W.L. (1994) Time-resolved detection of structural changes during the photocycle of spin-labeled bacteriorhodopsin, *Science* **266**, 105–107.

Subczynski, W.K., Hyde, J.S. (1981) The diffusion-concentration product of oxygen in lipid bilayers using the spin-label T_1 method, *Biochim. Biophys. Acta* **643**, 283–291.

Subczynski, W.K., Kusumi, A. (2003) Dynamics of raft molecules in the cell and artificial membranes: approaches by pulse EPR spin labeling and single molecule optical microscopy, *Biochim. Biophys. Acta Biomembr.* **1610**, 231–243.

Swamy, M.J., Ramakrishnan, M., Angerstein, B., Marsh, D. (2000) Spin-label electron spin resonance studies on the mode of anchoring and vertical location of the N-acyl chain in N-acylphosphatidylethanolamines, *Biochemistry* **39**, 12476–12484.

Thomas, C.E., Ohlweiler, D.F., Kalyanaraman, B. (1994) Multiple mechanisms for inhibition of low density lipoprotein oxidation by novel cyclic nitrone spin traps, *J. Biol. Chem.* **269**, 28055–28061.

Tommos, C., Tang, X.-S., Warncke, K., Hoganson, C.W., Styring, S., McCracken, J., Diner, B., Babcock, G.T. (1995) Spin-density distribution, conformation, and hydrogen bonding of the redox-active tyrosine Yz in photosystem II from multiple electron magnetic-resonance spectroscopies: implications for photosynthetic oxygen evolution, *J. Am. Chem. Soc.* **117**, 10325–10335.

Török, M., Milton, S., Kayed, R., Wu, P., McIntire, T., Glabe, C.G., Langen, R. (2002) Structural and dynamic features of Alzheimer's A peptide in amyloid fibrils studied by site-directed spin labeling, *J. Biol. Chem.* **277**, 40810–40815.

Trofanchuk, O., Stein, M., Geßner, Ch., Lendzian, F., Higuchi, Y., Lubitz, W., Miyazaki, F. (2000) Single crystal EPR studies of the oxidized active site of [NiFe] hydrogenase from *Desulfovibrio vulgaris*, *J. Biol. Inorg. Chem.* **5**, 36–44.

Willingham, G.L., Gaffney, B.J. (1983) Reactions of spin label cross-linking reagents with red blood cell proteins, *Biochemistry* **22**, 892–898.

Wu, F., Katsir, L.J., Seavy, M., Gaffney, B.J. (2003) Role of radical formation at Y193

in the allene oxide synthase domain of a lipoxygenase-AOS fusion protein from coral, *Biochemistry* **42**, 6871–6880.

Yonetani, T., Tsuneshige, A., Zhou, Y., Chen, X. (1998) Electron paramagnetic resonance and oxygen binding studies of -nitrosyl hemoglobin. A novel oxygen carrier having NO-assisted allosteric functions, *J. Biol. Chem.* **273**, 20323–20333.

Zweier, J.L., Samouilov, A., Kuppusamy, K. (1999) Non-enzymatic nitric oxide synthesis in biological systems, *Biochim. Biophys. Acta* **1411**, 250–262.

Zweier, J.L., Wang, P., Periannan Kuppusamy, P. (1995) Direct measurement of nitric oxide generation in the ischemic heart using electron paramagnetic resonance spectroscopy, *J. Biol. Chem.* **270**, 304–307.